

RESEARCH ARTICLE | JANUARY 10 2019

# Preparation of balsa-Nanosilver anti-infective eco-friendly dressing and its effect on wound healing **FREE**

Daijun Zhou; Tao Yang; Gaoxing Luo 

 Check for updates

*AIP Conf. Proc.* 2058, 020004 (2019)

<https://doi.org/10.1063/1.5085517>



View Online



Export Citation

CrossMark

## Articles You May Be Interested In

Preparation and evaluation of translucent Balsa-Caffeic acid modified lysozyme dressing

*AIP Conference Proceedings* (January 2019)

Preparation of chitin-lysozyme anti-infective eco-friendly dressing and its effect on wound healing

*AIP Conference Proceedings* (January 2019)

Synthesis of nanosilver, organophosphate ( $C_{10}H_{19}O_6PS_2$ ), and carbamate ( $CO_2NH_3$ ) for anopheles larva control in malaria endemic area on Covid-19 pandemic

*AIP Conference Proceedings* (May 2023)

500 kHz or 8.5 GHz?  
And all the ranges in between.

Lock-in Amplifiers for your periodic signal measurements



Find out more

 Zurich Instruments

# Preparation of Balsa-Nanosilver Anti-infective Eco-friendly Dressing and Its Effect on Wound Healing

Daijun Zhou<sup>1, a)</sup>, Tao Yang<sup>1)</sup>, Gaoxing Luo<sup>1, b)</sup>

<sup>1</sup>*Institute of Burn Research; State Key Laboratory of Trauma, Burn and Combined Injury; Key Laboratory of Proteomics of Chongqing, Southwest Hospital, Third Military Medical University, Chongqing 400038, China.*

<sup>a)</sup>Daijunzhou@vip.qq.com

<sup>b)</sup>Corresponding author email: jzdxl@qq.com

**Abstract.** This study aimed to prepare an anti-infective Eco-friendly dressing of balsa-Nanosilver, which should have antibacterial activity in vitro and promote wound healing in vivo. The balsa-Nanosilver was prepared using delignification (group Control) and dopamine gule(group A) methods respectively, at 1mmol/L, 2mmol/L, 4mmol/L (Namely group B, C and D). Finally, The Balsa-Nanosilver was observed as Nanosilver spherical particles and bedding dopamine colloid. FTIR showed that the Nanosilver had been adhered and the contact angle test showed that the material was still very hydrophilic. In vitro antibacterial effect was significant on *E. coli* and *S. aureus*. The cytotoxicity of the balsa-Nanosilver dressing was not found until day 7. On day 7, the healing rates were 34.5%, 40.8%, 57.9%, 69.3% and 73.5% in Group Control, A, B, C and D, respectively. The wound healing rate was higher in the C and D groups than these in the other three groups ( $P < 0.05$ ).

**Key words:** Balsa; Nanosilver; Wound Healing; Anti-infective Dressing.

## INTRODUCTION

As a renewable resource, wood has characteristics of low density, high modulus, high strength, high toughness and low thermal conductivity (Oliver et al., 2015). The balsa is the lightest commodity timber, due to its minimum dissolved heavy, material uniformity, low thermal conductivity (Stacy et al., 2012), and wonderful volume stability. balsa can do a variety of special structures (Payam et al., 2015) (Wang et al., 2016). At present, researches on the balsa wood by delignification suggested that the light transmittance could reach 90%, when it maintain the cellulose structure of the new transparent light fiber wood (Li et al., 2016). When applied as the wound dressing base material, it may have the effect of low cost, good air permeability and may be commonly used. Wound dressings containing AgNPs can effectively protect an injury from bacterial infection and promote tissue regeneration during the wound healing process. However, AgNPs are toxic to eukaryotes, and the cytotoxicity of such dressings should be taken into serious consideration. Clinically, it is often used in combination with other antimicrobial agents.

To date, the combination of Nanosilver and wound dressing has become a popular research field. Therefore, we will combine delignification balsa and Nanosilver to design a new economic and efficient antimicrobial dressing, and then assess its antibacterial activity in vitro, as well as its cytotoxicity and the effect on wound healing.

## MATERIALS AND METHODS

### Delignification

The balsa wood with the density about 160 kg/m<sup>3</sup> were punched and produced discs (diameter 0.6mm, thickness 0.8 mm). The discs were dried at 105 ± 3 ° C for 24 hours and then immersed in 1% the NaClO<sub>2</sub>-acetate buffer (pH

6.4, 80 °C) for 12 h. The samples were carefully washed with deionized water and then washed three times. Then dehydration was performed by ethanol: ethanol and acetone-acetone (1: 1) solution via three steps (10 min each step).

### **Dopamine Glue with Nanosilver**

Tris hydrochloric acid (131.14 mg) was solved in 100 ml of deionized water, and then 200 mg of dopamine powder was added to prepare a Tris-dopamine solution (2 mg / ml, pH 8.5). The balsa was then immersed in the dopamine solution for 12 h, placed in a shaker at 37 °C (100 rpm). Nanosilver powder(334mg) was dissolved in 200 ml of deionized water and generated as 10mmol/L Nanosilver solution, and then diluted to 1, 2and 4 mmol/L. The samples were washed with deionized water carefully, immersed in different concentrations of Nanosilver solution for 12 h on a 37°C shaker (100 rpm).

### **Scanning Electron Microscopy (SEM)**

The sample of the material wafer was carefully washed with deionized water, dried and sprayed, and the aperture structure of the film was observed under vacuum condition by scanning electron microscope and photographed.

### **Fourier Infrared Spectrum**

Different materials characterization and chemical structure was Testing by Fourier transform infrared spectroscopy (Nicolet-460 Thermo Fisher) ,wavenumber scan range is 600-4000 cm-1.

### **Contact Angle Test**

The film of different materials is placed on the horizontal surface, and the 1ul deionized water is dripped down from the top to the surface of the material. The contact angle size of the droplet is measured, and the average value of each sample is measured 3 times.

### **Tensile Property Test**

The tensile properties of the films were examined by universal material testing machine. The tensile strength and elongation at break were recorded as two indexes. The operating procedure is as follows:

Drying sample: width 10mm, total length 150mm, initial distance between clamps 100mm, standard distance length 50mm. The thickness is <1mm and the thickness is measured with micrometer (5 points per sample). Test speed 50mm/min, for testing. Each sample was subjected to 3 parallel tests and statistical analysis was carried out.

Swelling sample: soak the dried sample in PBS buffer (0.05mol/L, PH7.4) and swell 1h. After removal, the surface moisture is removed by filter paper, cut into dried samples, tested for the same shape, and measured with the same parameters

### **Drug Loading and Encapsulation Efficiency**

- (1) determination of nanosilver standard curve
- (2) determination of drug loading and encapsulation efficiency

Drug loading = actual nanosilver concentration \* volume (UG) / dissolved balsa-nanosilver total mass (mg);  
Encapsulation efficiency = actual nanosilver concentration / theoretical nanosilver concentration

### **Bacteria Co-Culture**

S.aureus and E.coli strains were obtained from the Institute of Burns, Southwest Hospital, Third Military Medical University. The bacteria (1\*104 CFU/ml) were first detected by the microplate reader (An OD value about 0.07 met the standard) and then added 200 ul into each well of the 96-well plates. Each group of materials was placed in the wells. Incubation was performed at 37 °C for 12 h and 24 h.

## Assay of Cytotoxicity

Normal neonatal mice were used to isolate primary fibroblasts as routine method,(reference) and the 3rd passage cells were used to assay the cytotoxicity of the prepared Balsa-Nanosilver dressing. After cells attached, materials were placed into wells. Each group contained 12 wells (for day 1, 3, 5 and 7 cell proliferation assessment, triple for each time point). Each well had 150 ul medium and cells were cultured in the 37°C incubator.

## Wound Healing Rate Assessment

Wound healing rate was calculated as follow. The wound area was measured by IPP6.0 software. Wound healing rate = (original wound area - residual wound area after injury) / original wound area x 100%.

## RESULTS

### Electron Microscopy Scanning and Tensile Tests

As shown in Figure. 1, the balsa retained the ordinary wood structure under Control1-3 was clear and complete. The balsa-Nanosilver group showed some deposition under D1 and D2.at higher magnification (D3, 2 x 104) the Paving dopamine layer and pellets Nanosilver were visible.

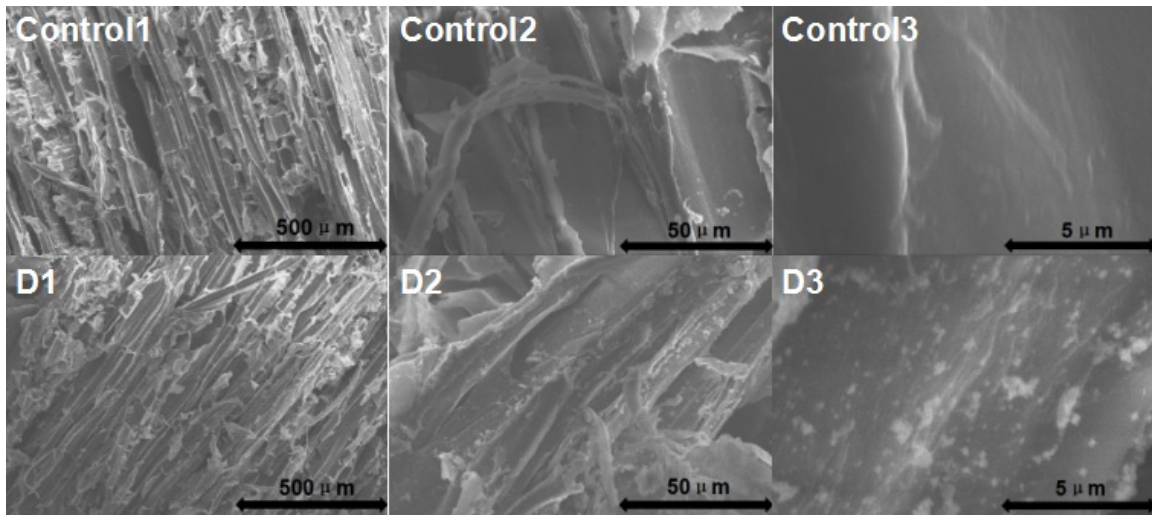
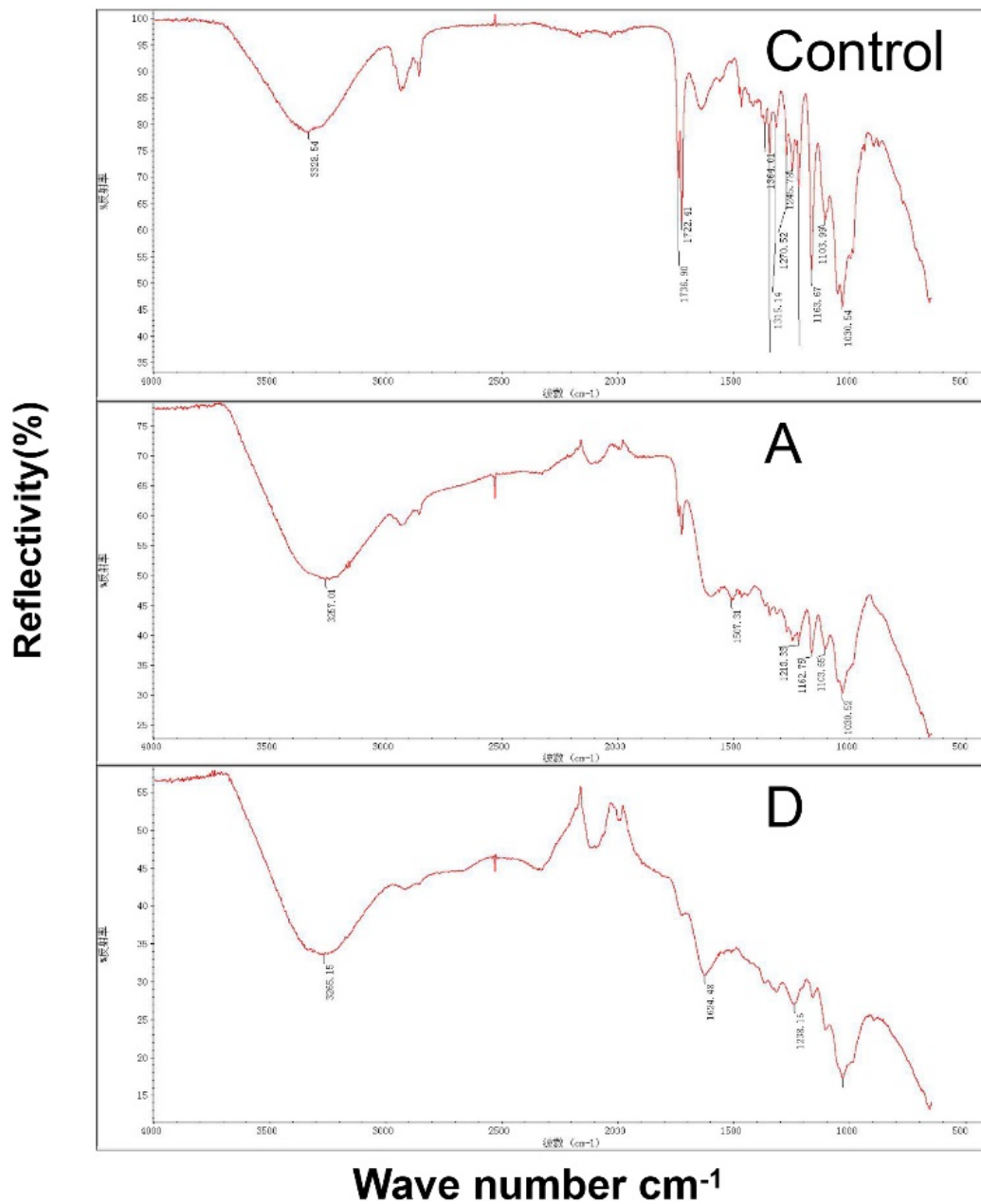


FIGURE 1. A is the delignification Control,D is 4mmol/L balsa-Nanosilver

### Fourier Infrared Spectrum

As shown in Figure 2,The infrared spectra of the 3 groups (Control,A,D) were approximately similar, and about 3328.54cm<sup>-1</sup>,3257.01cm<sup>-1</sup>,3265.15cm<sup>-1</sup> were the O-H stretching vibration peaks of hydroxyl groups in wood fibers;The absorption peak at 1736.90cm<sup>-1</sup>,1722.41cm<sup>-1</sup> in untreated wood fiber is the stretching vibration of C-O-C in C-O. After surface modification, the peak shifts to near 1507.31cm<sup>-1</sup> because of the introduction of C=O structure.As shown in D, Nanosilver has two distinct characteristic peaks, 1624.48cm<sup>-1</sup> and 1238.16cm<sup>-1</sup>.



**FIGURE 2.** The infrared spectra of the Control,A and D groups

### Contact Angle Test

As shown in Figure 3, the average contact angle ( $\theta$ ) of Control group is  $3.90 \pm 0.85^\circ$ , A is  $4.39 \pm 0.91^\circ$ , D is  $5.38 \pm 1.02^\circ$ . Compared with A and D, the difference was not statistically significant ( $P > 0.05$ ).

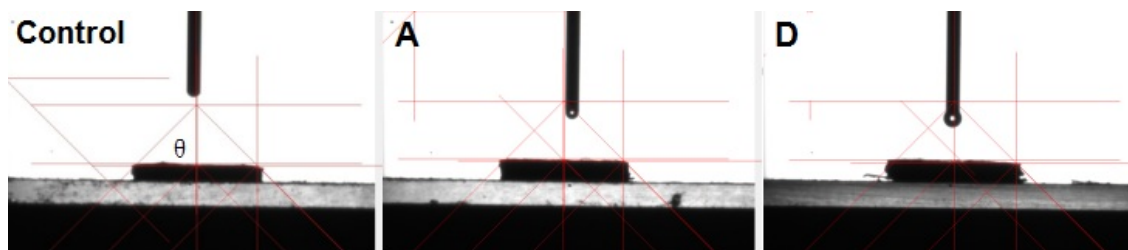


**FIGURE 3.** The average contact angle ( $\theta$ ) of Control group is  $3.90 \pm 0.85^\circ$ , A is  $4.61 \pm 1.17^\circ$ , D is  $19.46 \pm 4.21^\circ$

### Enzyme Loading and Encapsulation Efficiency

As shown in Table 1, with the increasing of Nanosilver concentration, the drug loading rate of Chitin-lysozyme increased gradually, while encapsulation efficiency decreased gradually ( $P < 0.05$ ).

**TABLE 1.** Drug loading and encapsulation efficiency of Balsa-Nanosilver in different groups

	B	C	D
Drug loading ( $\mu\text{g}/\text{mg}$ )	$29.7 \pm 3.2$	$43.6 \pm 4.7$	$59.7 \pm 5.8$
Encapsulation efficiency (%)	$76.8 \pm 5.9$	$68.2 \pm 5.1$	$53.4 \pm 4.0$

### Release in Vitro

As shown in Figure 4, the release rate of B, C and D groups tended to be stable and maximum at 48h, and the cumulative release percentages were 78.2%, 86.3% and 87.0% after 72h.

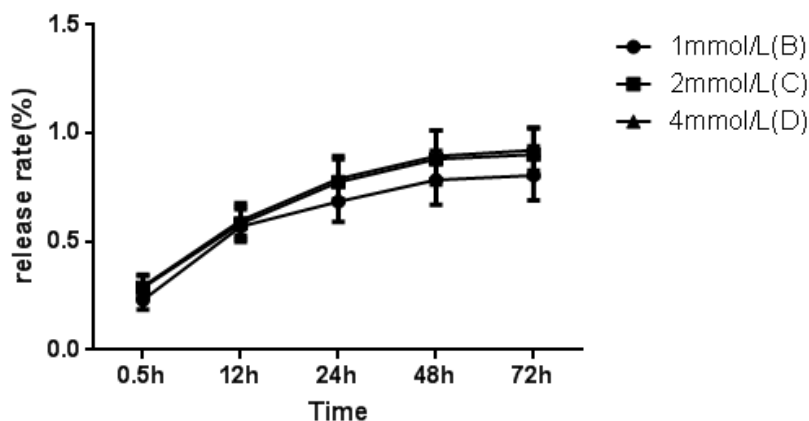


**FIGURE 4.** drug release in vitro of different concentrations of wood-lysozyme

### Tensile Property Test

As shown in Table 1, In dry state, the excellent degree of tensile strength and elongation at break is Control < A < B < C < D. In the swelling state, the tensile strength and elongation at break of each group are improved.

**TABLE 2.** The Tensile property test of chitin-lysozyme

	Dry state		Swollen state	
	Tensile strength (MPa)	Elongation at break (%)	Tensile strength (MPa)	Elongation at break (%)
Control	21.7±3.0	11.6±0.5	26.3±3.4	13.2±0.9
A	32.8±3.7	15.3±1.2	36.7±3.9	17.2±1.7
B	41.8±4.1	19.7±1.6	45.8±4.3	21.8±1.9
C	49.4±4.9	25.6±2.0	52.8±5.4	28.0±2.1
D	55.6±5.4	29.3±2.3	59.0±5.8	31.7±2.6

### Assay of the Antibacterial Activity

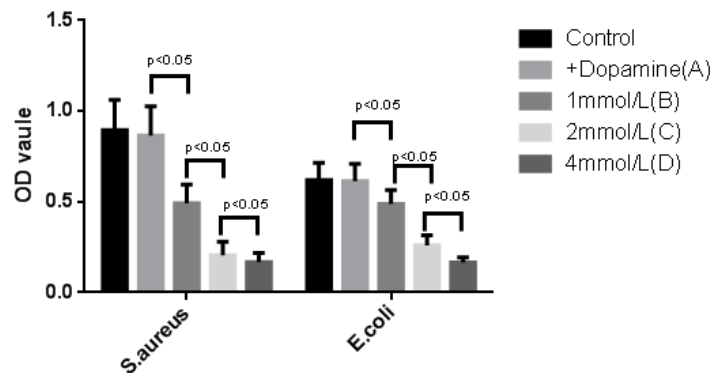
As shown in Table3,4 and Figure. 5, compared with the control group , the inhibitory effect on the bacteria was gradually increased when the concentration of Nanosilver increased. The difference between each two groups was statistically significant (P <0.05).

**TABLE 3.** OD values of co-culture of different concentrations of balsa-Nanosilver dressings and *S.aureus*.

	Control	A	B	C	D
12h	0.628±0.120	0.622±0.118	0.418±0.107	0.269±0.068	0.187±0.056
24h	0.895±0.167	0.866±0.160	0.492±0.114	0.205±0.075	0.167±0.051

**TABLE 4.** OD values of co-culture of different concentrations of balsa-Nanosilver dressings and *E.coli*.

	Control	A	B	C	D
12h	0.503±0.082	0.489±0.081	0.362±0.065	0.233±0.051	0.139±0.032
24h	0.619±0.097	0.614±0.095	0.417±0.060	0.259±0.057	0.165±0.029

**FIGURE 5.** The inhibitory effects on the bacteria was gradually increased with the concentration of Nanosilver (P <0.05)

## Test of Cytotoxicity

As shown in Table 5 and Figure. 6, Nanosilver in different concentrations was hardly inhibited the cell growth ( $P > 0.05$ ). Only on day 7, group C, D showed a light inhibitory effect ( $P < 0.05$ ).

**TABLE 5.** Cytotoxicities of different concentrations of balsa-Nanosilver dressings on the mice fibroblasts

	1Day	3Day	5Day	7Day
Control	0.268±0.029	0.395±0.037	0.590±0.058	0.778±0.070
A	0.266±0.028	0.390±0.034	0.601±0.060	0.751±0.072
B	0.272±0.031	0.387±0.035	0.589±0.056	0.749±0.068
C	0.279±0.035	0.392±0.036	0.556±0.054	0.675±0.062
D	0.273±0.031	0.379±0.041	0.548±0.052	0.660±0.059

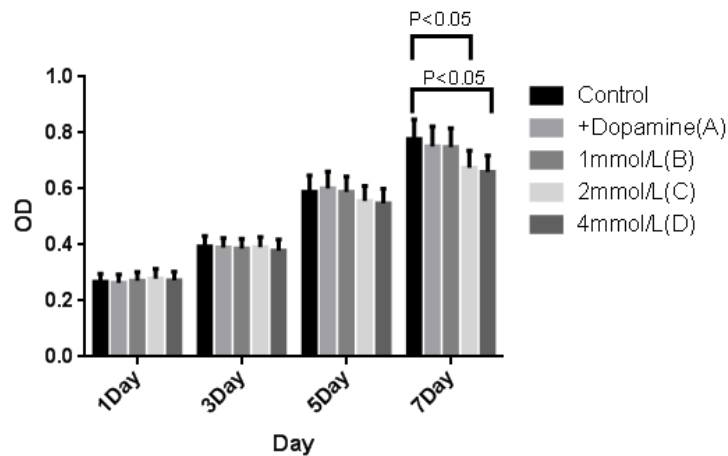


**FIGURE 6.** Until day 7, group D had inhibitory effect on cell proliferation ( $P < 0.05$ )

## Effect on Infectious Wound Healing

On day 7, the healing rates were 34.5%, 40.8%, 57.9%, 69.3% and 73.5% in Group Control, A, B, C and D, respectively. The wound healing rate was higher in the C and D groups than these in the other three groups ( $P < 0.05$ ). The difference between the C and D groups was not significant ( $P > 0.05$ ).

## DISCUSSION

As a natural renewable wood, balsa has a low density, high elastic modulus, high strength, high toughness and low thermal conductivity (Stacy et al., 2012) (Etienne et al., 2014). It has been suggested that the removal of the strongly absorbable delignification by the specific method of polymerizing formaldehyde methyl acrylate can increase the light-wood transmittance by 85%, thereby reducing the balsa wood thickness and fiber volume fraction, with good structural mechanical properties and optical translucency appearance (Li et al., 2016).

The ideal wound dressings should have the following characteristics: good mechanical properties, proper water vapor permeability and fine biocompatibility (Guo and Dipietro, 2010). More importantly, infection, inflammation, etc. will cause a slow down or failure of the wound healing, the ideal wound dressing should also be able to provide a local surface suitable for antibacterial effect (Morsy et al., 2016) (Leslie et al., 2015). The natural materials such as chitin and chitosan, dextran, cellulose, alginate, silk protein, etc. have been considered good wound dressings materials,



because of their biocompatibility. It has thus become a hot topic to use natural materials loaded with antibacterial agents, growth factors or other chemicals, to promote the healing of infectious wounds (Dreifke et al, 2015) (Wang et al, 2016).

As shown in Figure 2, the balsa retained the ordinary wood structure under Control 1-3 was clear and complete. The wood texture is clear, consistent with previous studies (Li et al., 2016) (Zhu et al., 2016). The balsa-Nanosilver group showed some deposition under D1 and D2. At higher magnification (D3, 2 x 104) the Paving dopamine layer and pellets Nanosilver were visible. We think that is because the Nanosilver concentration of 4 mmol/L is much larger than other reports. As shown in Figure 3, The infrared spectra of the 3 groups (Control, A, D) were approximately similar, and about 3328.54 cm<sup>-1</sup>, 3257.01 cm<sup>-1</sup>, 3265.15 cm<sup>-1</sup> were the O-H stretching vibration peaks of hydroxyl groups in wood fibers; The absorption peak at 1736.90 cm<sup>-1</sup>, 1722.41 cm<sup>-1</sup> in untreated wood fiber is the stretching vibration of C=O in C-O. After surface modification, the peak shifts to near 1507.31 cm<sup>-1</sup> because of the introduction of C=O structure. As shown in D, Nanosilver has two distinct characteristic peaks, 1624.48 cm<sup>-1</sup> and 1238.16 cm<sup>-1</sup>. It shows that the Nanosilver molecule has been immobilized on the carrier, but the secondary structure has not changed significantly.

As shown in Figure 4, the average contact angle ( $\theta$ ) of Control group is 3.90 ± 0.85°, A is 4.39 ± 0.91°, D is 5.38 ± 1.02°. Compared with A and D, the difference was not statistically significant (P > 0.05), it still has hydrophilicity. As shown in Table 1 and Figure 5, with the increasing of Nanosilver concentration, the drug loading rate of Chitin-lysozyme increased gradually, while encapsulation efficiency decreased gradually (P < 0.05). The release rate of B, C and D groups tended to be stable and maximum at 48h, and the cumulative release percentages were 78.2%, 86.3% and 87.0% after 72h. As shown in Table 2, In dry state, the excellent degree of tensile strength and elongation at break is Control < A < B < C < D. In the swelling state, the tensile strength and elongation at break of each group are improved. As shown in Table 3, 4 and Figure 5, compared with the control group, the inhibitory effect on the bacteria was gradually increased when the concentration of Nanosilver increased. The difference between each two groups was statistically significant (P < 0.05). And as shown in Table 5 and Figure 6, Nanosilver in different concentrations was hardly inhibited the cell growth (P > 0.05). Only on day 7, group C, D showed a light inhibitory effect (P < 0.05). It is proved that nano silver has both high antibacterial activity and low toxicity.

The defense barrier on body surface of the burns were destroyed, and the immune capacity decreased significantly. Extensive tissue necrosis and invasion of bacteria in vivo will lead to wound infection (Fournier et al, 2015). Wound infection is one of the major complications and key cause of death in burned patients. About 52% -70% of burns die due to wound infection (Keisuke et al, 2015). In this study, bacterial concentrations were 108/ml (Costley et al, 2017). The healing rates were 34.5%, 40.8%, 57.9%, 69.3% and 73.5% in Group Control, A, B, C and D, respectively. The wound healing rate was higher in the C and D groups than these in the other three groups (P < 0.05). The difference between the C and D groups was not significant (P > 0.05). The results suggest that the anti-infective effect no more increases but when the concentration reaches a certain level (2 mmol/L).

In summary, this study prepared a natural balsa-Nanosilver anti-infective dressings in different concentrations; and concentrations of 2-4 mmol/L were effective. Balsa-Nanosilver dressing promoted wound healing. High concentration with long-term contact might inhibit cell proliferation. This dressing provides a new means for wound healing via natural materials.

## REFERENCES

1. Vay O., Borst KD., Hansmann C., Teischinger A., Müller U., 2015, Thermal conductivity of wood at angles to the principal anatomical directions, *Wood Science and Technology*, 49, 577-589, DOI: 10.1007/s00226-015-0716-x.
2. Trey S., Jafarzadeh S, Johansson, M., 2012, in situ Polymerization of Polyaniline in Wood Veneers. *ACS Appl Mater Interfaces*, 3, 1760-9, DOI: 10.1021/am300010s.
3. Nejat P, Jomehzadeh F., Taheri MM., Gohari M., Majid MZA, 2015, A global review of energy consumption, CO2 emissions and policy in the residential sector (with an overview of the top ten CO2 emitting countries), *Renewable Sustainable Energy Rev*, 43, 843-862, DOI: 10.1016/j.rser.2014.11.066.
4. Sen W., Ang L., Lina Z, 2016, Recent advances in regenerated cellulose materials, *Prog Polym Sci*, 53, 169 - 206, DOI: 10.1016/j.progpolymsci.2015.07.003.
5. Li Y., Fu Q., Yu S., Yan M., Berglund L, 2016, Optically Transparent Wood from a Nanoporous Cellulosic Template, Combining Functional and Structural Performance, *Biomacromolecules*, 17, 1358-64, DOI: 10.1021/acs.iomac.6b00145.

6. Cabane E.,Keplinger T.,Kunniger T.,Merk V.,Burgert I,2014,Functional lignocellulosic materials prepared by ATRP from a wood scaffold,[ChemSusChem](#),7,1020-1025,DOI:10.1038/srep31287.
7. Guo S.,Dipietro LA,2010,Factors affecting wound healing,[J Dent Res](#), 89, 219-29, DOI: 10. 1177/0022034509359125.
8. Morsy R.,Hosny M.,Reicha F.,Elnimn T,2016,Development and characterization of multifunctional electrospun ferric oxide-glue-glycerol nanofibrous mat for wound dressing applications,[Fibers and Polymers](#),42,578 - 582,DOI: 10.1007/s12221-016-6915-8.
9. Chan LW.,Kim CH.,Wang X.,Pun SH.,White NJ.,Kim TH,2016,PolySTAT-modified chitosan gauzes for improved hemostasis in external hemorrhage,[Acta Biomater](#),31,178–185,DOI:10.1016/j.actbio.2015.11.017
10. Dreifke MB.,Jayasuriya AA.,Jayasuriya A,2015,CCurrent wound healing procedures and potential care,[Mater Sci Eng C Mater Biol Appl](#),48, 651–662,DOI:10.1016/j.msec.2014.12.068.
11. Wang Y.,Xu R.,Luo G.,Lei Q.,Shu Q.,Yao Z.,Li H.,Zhou J.,Tan J.,Yang S.,Zhan R.,He W.,Wu J,2016,Biomimetic fibroblast-loaded artificial dermis with "sandwich" structure and designed gradient pore sizes promotes wound healing by favoring granulation tissue formation and wound re-epithelialization, [Acta Biomater](#),30,246–257,DOI:10.1016/j.actbio.2015.11.035.
12. Zhu M., Song J.,Li T.,Gong A.,Wang Y.,Dai J.,Yao Y.,Luo W.,Henderson D.,Hu L,2016,Highly Anisotropic, Highly Transparent Wood Composites,[Adv Mater](#),28,5181-5187,DOI:10.1002/adma.201604084.
13. Fournier A.,Eggimann P.,Pagani J L.,Revelly J P.,Decosterd LA.,Marchetti O.,Pannatier A.,Voirol P.,Que YA,2015,Impact of the introduction of real-time therapeutic drug monitoring on empirical doses of carbapenems in critically ill burn patients,[Burns](#),41,956-968,DOI:956-68,10.1016/j.burns.2015.01.001.
14. Ito K., Saito A.,Fujie T.,Nishiwaki K.,Miyazaki H.,Kinoshita M.,Saitoh D.,Ohtsubo S.,Takeoka S, 2015, Sustainable antimicrobial effect of silver sulfadiazine-loaded nanosheets on infection in a mice model of partial-thickness burn injury,[Acta Biomater](#),24,87-95,DOI:10.1016/j.actbio.2015.05.035
15. Costley D.,Nesbitt H.,Ternan N.,Dooley J.,Huang Y Y.,Hamblin MR.,McHale AP.,Callan JF, 2017, Sonodynamic inactivation of Gram-positive and Gram-negative bacteria using a Rose Bengal-antimicrobial peptide conjugate,[Int J Antimicrob Agents](#),49,31-36,DOI:10.1016/j.ijantimicag.2016.09.034.